BIOLOGICAL CRYSTALLOGRAPHY
ISSN 1399-0047

Structure of the DNA-binding domain of the response regulator SaeR from *Staphylococcus aureus*

Xiaojiao Fan,[a,b]‡ Xu Zhang,[a,c]‡ Yuwei Zhu,[a,b] Liwen Niu,[a,b] Maikun Teng,[a,b]* Baolin Sun[a,c]* and Xu Li[a,b]*

[a]Hefei National Laboratory for Physical Sciences at Microscale and School of Life Sciences, University of Science and Technology of China, Hefei, Anhui 230026, People's Republic of China, [b]Key Laboratory of Structural Biology, Chinese Academy of Sciences, Hefei, Anhui 230026, People's Republic of China, and [c]CAS Key Laboratory of Innate Immunity and Chronic Disease, School of Life Sciences and Medical Center, University of Science and Technology of China, Hefei, Anhui 230026, People's Republic of China. *Correspondence e-mail: mkteng@ustc.edu.cn, sunb@ustc.edu.cn, sachem@ustc.edu.cn

Received 8 December 2014
Accepted 28 May 2015

Edited by Q. Hao, University of Hong Kong

‡ These authors contributed equally to this work.

Keywords: *Staphylococcus aureus*; TCS; SaeR; DNA-binding domain.

PDB reference: DNA-binding domain of SaeR, 4qwq

Supporting information: this article has supporting information at journals.iucr.org/d

The SaeR/S two-component regulatory system is essential for controlling the expression of many virulence factors in *Staphylococcus aureus*. SaeR, a member of the OmpR/PhoB family, is a response regulator with an N-terminal regulatory domain and a C-terminal DNA-binding domain. In order to elucidate how SaeR binds to the promoter regions of target genes, the crystal structure of the DNA-binding domain of SaeR ($SaeR^{DBD}$) was solved at 2.5 Å resolution. The structure reveals that $SaeR^{DBD}$ exists as a monomer and has the canonical winged helix–turn–helix module. EMSA experiments suggested that full-length SaeR can bind to the P1 promoter and that the binding affinity is higher than that of its C-terminal DNA-binding domain. Five key residues on the winged helix–turn–helix module were verified to be important for binding to the P1 promoter *in vitro* and for the physiological function of SaeR *in vivo*.

1. Introduction

Staphylococcus aureus is an important human pathogen that can cause diseases ranging from mild to life-threatening (Lowy, 1998). Some severe syndromes or pathologies including pneumonia, sepsis and endocarditis have been compounded by the emergence of methicillin-resistant and vancomycin-resistant *S. aureus* (Gillet *et al.*, 2002; Adem *et al.*, 2005; Miller *et al.*, 2005; Cosgrove *et al.*, 2004). The diversity and severity of these diseases depend on the expression of virulence factors in *S. aureus*. The coordinated temporal expression of these virulence factors is tightly regulated by many regulatory elements including global regulators (for example SigB, SarA and SarA homologues), two-component regulatory systems (for example *agr*, *saeRS* and *arlRS*) and regulatory RNA molecules (for example RNAIII) (Bischoff *et al.*, 2004; Cheung *et al.*, 2008; Giraudo *et al.*, 1997; Fournier *et al.*, 2001; Arvidson & Tegmark, 2001; Cheung & Ying, 1994; Morfeldt *et al.*, 1996).

Two-component regulatory systems (TCSs) exhibit a signal transduction mechanism by which bacteria, lower eukaryotes and plants monitor and respond to environmental conditions (Wuichet *et al.*, 2010). *S. aureus* harbours 16 conservative TCSs (Jeong *et al.*, 2011), which are involved in the regulation of biofilm formation, capsular polysaccharide synthesis, autolysis, antibiotic resistance and haem toxin resistance (Xue *et al.*,

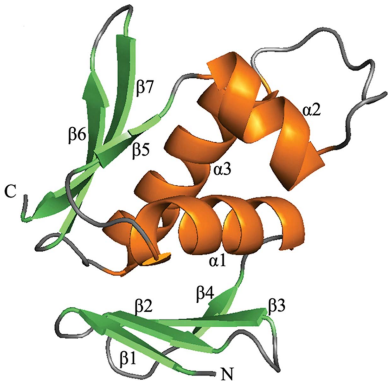

2011; Brunskill & Bayles, 1996; Gardete *et al.*, 2006; Hiron *et al.*, 2011). As TCSs are absent in mammals and play a role in virulence, they have been envisaged to be valid targets for the development of new antimicrobials (Barrett & Hoch, 1998; Stephenson & Hoch, 2002). In general, a TCS consists of a sensor histidine kinase (HK) and response regulator (RR) (Hoch, 2000). On receiving a signal, the HK autophosphorylates and the phosphate group is then transferred to a conserved Asp residue in the RR (Stock *et al.*, 2000). The phosphorylation of the RR most often alters its DNA-binding activity, which leads to changes in gene expression (Hoch, 2000; West & Stock, 2001). The RR has a conserved receiver domain (RD) and a variable output domain (Galperin, 2006). About two-thirds of output domains bind to DNA; the remainder includes enzymatic domains, domains with protein-binding ability and some domains of unknown function (Galperin, 2006).

The *sae* (***S***. ***a****ureus* **e**xoprotein expression) locus consists of four genes, *saeP*, *saeQ*, *saeR* and *saeS* (Novick & Jiang, 2003), among which *saeS* and *saeR* encode the sensor HK and the RR, acting as a TCS (Giraudo *et al.*, 1999). The SaeR/S TCS plays a key regulatory role in the expression of many virulence factors, including some secreted proteins (for example Coa, Hla and Hlb), cell-wall proteins (for example Spa and FnbA) and cell wall-associated proteins (for example Eap and Emp) (Giraudo *et al.*, 1994, 1997; Goerke *et al.*, 2005; Harraghy *et al.*, 2005). Additionally, SaeR/S has a more complicated transcriptional pattern that is profoundly influenced by *agr* and by certain environmental stimuli (*e.g.* 1 *M* NaCl, a pH below 6 or subinhibitory clindamycin; Novick & Jiang, 2003).

SaeR belongs to the OmpR/PhoB subfamily of response regulators. It contains an N-terminal receiver domain and a C-terminal DNA-binding domain (DBD) that recognizes motifs near the promoter sequences of target genes (Giraudo *et al.*, 1999; Steinhuber *et al.*, 2003). To date, seven structures of full-length response regulators from the OmpR/PhoB family have been deposited in the Protein Data Bank: DrrB (Robinson *et al.*, 2003) and DrrD (Buckler *et al.*, 2002) from *Thermotoga maritima*, PrrA (Nowak *et al.*, 2006), MtrA (Friedland *et al.*, 2007), RegX3 (King-Scott *et al.*, 2007) and PhoP (Menon & Wang, 2011) from *Mycobacterium tuberculosis*, and KdpE (Narayanan *et al.*, 2014) from *Escherichia coli*. Comparison of these structures suggests that the DNA-binding domain can exist in two types of conformation: closed and open. The DrrB (Robinson *et al.*, 2003), DrrD (Buckler *et al.*, 2002), RegX3 (King-Scott *et al.*, 2007), PhoP (Menon & Wang, 2011) and KdpE (Narayanan *et al.*, 2014) structures have the DNA-binding elements fully exposed, showing that they are able to bind to DNA without phosphorylation. In contrast, MtrA (Friedland *et al.*, 2007) and PrrA (Nowak *et al.*, 2006) exhibit very compact structures with the recognition helix completely inaccessible to DNA. However, PrrA (Nowak *et al.*, 2006) can exist in an open conformation in order to bind DNA in solution without phosphorylation. Some structures of the receiver domains in complex with beryllium fluoride to mimic the phosphorylation-activated structure have been reported (Bachhawat & Stock, 2007; Bachhawat *et al.*, 2005; Toro-Roman *et al.*, 2005). These receiver domains dimerize using their $\alpha4$–$\beta5$–$\alpha5$ faces in the active state. Some receiver domains also form dimers through the same interface in the absence of phosphorylation (Bachhawat & Stock, 2007; Bachhawat *et al.*, 2005). Besides the RD structures, some DBD structures have also been reported, such as the DBD structures of PhoB (Blanco *et al.*, 2002), OmpR (Martínez-Hackert & Stock, 1997), KdpE (Narayanan *et al.*, 2012) from *E. coli* and PhoP (Wang *et al.*, 2007) from *M. tuberculosis*. They all contain a typical helix–turn–helix motif and a β-hairpin motif. All structures show monomers in the crystal except for PhoP, which exhibits a hexamer ring with neighbouring molecules interacting in a head-to-tail pattern (Wang *et al.*, 2007).

In order to elucidate how SaeR binds to the promoter regions of target genes, we determined the crystal structure of the DNA-binding domain of SaeR (referred to as $SaeR^{DBD}$) at 2.5 Å resolution. The structure reveals that $SaeR^{DBD}$ exists as a monomer and has the typical winged helix–turn–helix module. EMSA experiments showed that full-length SaeR had a higher binding affinity than that of $SaeR^{DBD}$. We also confirmed the vital role of several key residues in the winged helix–turn–helix module of SaeR in binding to P1 promoter DNA *in vitro* and the physiological function of SaeR *in vivo*. Finally, the putative $SaeR^{DBD}$–dsDNA recognition model is discussed.

2. Materials and methods

2.1. Cloning, expression and purification

The full-length SaeR (residues 1–228), $SaeR^{RD}$ (residues 3–136) and $SaeR^{DBD}$ (residues 125–228) genes were PCR-amplified from *S. aureus* strain NCTC 8325 using Prime STAR HS DNA polymerase (Takara). The DNA fragment was cloned into a modified pET-28a(+) vector with a 6×His tag using the NdeI/XhoI restriction sites. All SaeR mutations were generated using the MutanBEST kit (Takara). Overexpression of all recombinant proteins was induced in *E. coli* BL21 (DE3) cells (Novagen) using 0.5 m*M* isopropyl β-D-1-thiogalactopyranoside (IPTG) when the cell density reached an OD_{600} of 0.6–0.8. After growth for about 20 h at 289 K, the cells were collected and lysed. The recombinant proteins were purified using Ni^{2+}–nitrilotriacetate affinity resin (Ni–NTA, Qiagen) in buffer (50 m*M* Tris–HCl pH 7.5, 200 m*M* NaCl, 5% glycerol) and the 6×His $SaeR^{DBD}$ fusion protein was eluted with 200 m*M* imidazole. The proteins were further purified using HiTrap Q FF (5 ml) and HiLoad 16/60 Superdex 200 (GE Healthcare) columns. The proteins were concentrated to 29 mg ml^{-1} in buffer consisting of 20 m*M* Tris–HCl pH 7.5, 100 m*M* NaCl for crystallization trials.

2.2. Crystallization, data collection and structure determination

Crystals of $SaeR^{DBD}$ were grown using the hanging-drop vapour-diffusion method at 289 K and yielded crystals in 2 d when mixed in a 1:1 ratio with well solution consisting of 15% PEG 6K, 0.1 *M* bis-tris pH 6.2. The addition of 0.1 *M*

Table 1
Data-collection and refinement statistics for SaeR^{DBD}.

Values in parentheses are for the highest resolution shell.

Data-collection statistics	
Space group	$P2_12_12_1$
a, b, c (Å)	31.97, 62.65, 116.26
α, β, γ (°)	90, 90, 90
Wavelength (Å)	0.9791
Resolution limits (Å)	50.00–2.50 (2.59–2.50)
No. of unique reflections	8586
Completeness (%)	99.7 (100)
Multiplicity	13.8 (14.3)
R_{merge}† (%)	9.2 (49.5)
Mean $I/\sigma(I)$	34.3 (8.4)
Refinement statistics	
Resolution limits (Å)	31.32–2.50
R_{work}‡/R_{free}§ (%)	23.21/27.33
R.m.s.d., bond lengths (Å)	0.028
R.m.s.d., angles (°)	1.704
B factor (Å^2)	
Protein	60.67
H_2O	51.70
No. of non-H protein atoms	1585
No. of water O atoms	11
Ramachandran plot (%)	
Most favoured regions	84.4
Additional allowed regions	15.6
Generously allowed regions	0
PDB entry	4qwq

† $R_{merge} = \sum_{hkl}\sum_i |I_i(hkl) - \langle I(hkl)\rangle| / \sum_{hkl}\sum_i I_i(hkl)$, where $I_i(hkl)$ is the ith observation of reflection hkl and $\langle I(hkl)\rangle$ is the weighted average intensity for all i observations of reflection hkl. ‡ $R_{work} = \sum_{hkl} ||F_{obs}| - |F_{calc}|| / \sum_{hkl} |F_{obs}|$, where F_{obs} and F_{calc} are the observed and calculated structure factors for reflection hkl, respectively. § R_{free} was calculated in the same way as R_{work} but using a randomly selected 5% of the reflections which were omitted from refinement.

spermidine yielded larger crystals. For data collection, all crystals were soaked in a cryoprotectant solution consisting of the respective reservoir solution supplemented with 20%(*v*/*v*) glycerol and were then flash-cooled in liquid nitrogen. Data sets for all crystals were collected on beamline 17U at the Shanghai Synchrotron Radiation Facility (SSRF) at 100 K. The data were processed and scaled with the *HKL*-2000 package (Otwinowski & Minor, 1997) and programs from the *CCP*4 package (Winn *et al.*, 2011). The SaeR^{DBD} structure was determined by molecular replacement using *MOLREP* (Vagin & Teplyakov, 2010) from the *CCP*4 suite (Winn *et al.*, 2011). The structure of the DNA-binding domain of PhoB from *E. coli* (PDB entry 1gxq; Blanco *et al.*, 2002), which shows 31.8% identity to SaeR^{DBD}, was used as the search model. The initial model from *MOLREP* was refined to the full resolution range using *REFMAC*5 (Murshudov *et al.*, 2011), *PHENIX* (Adams *et al.*, 2010) and manual rebuilding in *Coot* (Emsley & Cowtan, 2004). TLS restraints were used in the last several cycles of refinement in *phenix.refine*. The final model was evaluated with *MolProbity* (Chen *et al.*, 2010) and *PROCHECK* (Laskowski *et al.*, 1993). The crystallographic parameters are listed in Table 1. All figures showing structures were prepared with *PyMOL*.

2.3. Electrophoretic mobility shift assay (EMSA)

An EMSA was performed as described previously (Xue *et al.*, 2014). The P1 promoter of the *sae* operon was PCR-amplified from *S. aureus* strain NCTC 8325 with a biotin-labelled primer P1-F (5′-TTGGTACTTGTATTTAATCGTC-TATC-3′) and P1-R (5′-GTTGTGATAACAGCACCAGC-3′). The DNA probe was mixed with increasing amounts of SaeR in a 10 µl reaction mixture consisting of 20 m*M* Tris–HCl pH 7.5, 100 m*M* NaCl, 0.5 µg poly(dI–dC) on ice for 30 min. After incubation, the mixtures were electrophoresed in 5% native polyacrylamide gel in 1× TBE buffer and then electro-transferred onto a charged nylon membrane (Millipore) in 0.5× TBE. The biotin-labelled probe was detected using the Chemiluminescent Nucleic Acid Detection Module (Pierce).

2.4. Size-exclusion chromatography assay

Size-exclusion chromatography was carried out using a Superdex 200 column (10/300 GL, GE Healthcare) attached to an ÄKTAprime plus (GE Healthcare). Briefly, protein samples or molecular-mass standards were applied onto the Superdex 200 column at a flow rate of 0.6 ml min^{-1} and eluted with 50 m*M* Tris–HCl pH 7.5, 100 m*M* NaCl. The standard proteins (GE Healthcare) used in this assay were β-amylase (200.0 kDa), alcohol dehydrogenase (150.0 kDa), albumin (66.0 kDa), carbonic anhydrase (29.0 kDa) and cytochrome *c* (12.4 kDa). The void volume was determined with blue dextran (GE Healthcare). Proteins were detected by the absorbance measured at 280 nm.

2.5. CD spectroscopy

Purified SaeR and its mutants (0.15 mg ml^{-1}) in 50 m*M* sodium phosphate buffer pH 7.5 were loaded into a quartz cuvette (d = 0.1 cm path length) and CD spectra were recorded from 190 to 260 nm on a Jasco J810 spectropolarimeter at 298 K. A buffer-only sample was used as a reference. All CD spectra represent the average of three successive spectra. The molar ellipticities (θ) were plotted *versus* wavelength and the reference curve was subtracted from each curve.

2.6. Complementation of the *saeR* knockout strain

The *saePQRS* knockout strain NMΔsae is an *S. aureus* Newman strain with the *sae* operon deleted, which was kindly provided by Dr Taeok Bae (Sun *et al.*, 2010). Complementation of the *saePQRS* knockout was achieved using a plasmid expressing the *saePQRS* operon under the control of its native promoter. The fragment of the *saePQRS* operon was amplified using primer pairs P671 (5′-AACGAATTCTTGGTACTTG-TATTTAATCGTCTATC-3′) and saeC-R (5′-GCGGGATC-CTGATGAGAAGGATACCCATA-3′) and cloned into the plasmid pLI50 (Addgene). The complementary plasmids of different SaeR mutants were generated using the MutanBEST kit (Takara) with the plasmid pLI50-*saePQRS* as a template. These recombinant plasmids were transformed into *S. aureus* RN4220 for modification and then transformed into wild-type and NMΔsae strains by electroporation.

2.7. Assays for the α-toxin

A Western blot of the α-toxin was performed as described previously (Zhu *et al.*, 2014). Briefly, the same amount of stationary-phase supernatant of different strains was collected and heated for 10 min at 368 K; the samples were then separated by SDS–PAGE and electrotransferred onto a polyvinylidene difluoride membrane (GE). The protein was detected by a rabbit anti-α-toxin antibody (Sigma) followed by horseradish peroxidase-conjugated sheep anti-rabbit antibodies (Pierce). Haemolysis was assayed by spotting 5 µl of an overnight culture onto sheep blood agar (Kailin, People's Republic of China) and incubating at 310 K for 3 d.

3. Results and discussion

3.1. The DNA-binding properties of SaeR and SaeR^{DBD}

The *saePQRS* operon is a key element in the regulatory cascade governing the staphylococcal virulon. The SaeR/S TCS upregulates many virulence factors, including secreted proteins such as haemolysin, coagulase, proteases *etc.* and some cell wall-associated proteins, and downregulates capsular polysaccharide (Giraudo *et al.*, 1994, 1997; Harraghy *et al.*, 2005; Li & Cheung, 2008; Arumugaswami *et al.*, 2009; Goerke *et al.*, 2005). SaeR acts as a transcriptional regulator and modulates the expression of target genes by directly binding to their promoters. How SaeR interacts with the promoter region of target genes, however, remains unknown. To investigate the DNA-binding properties of SaeR, the P1 promoter of the *sae* operon was chosen as the DNA-binding substrate because the promoter is strongly autoregulated by *sae* (Geiger *et al.*, 2008). As shown in Fig. 1(*a*), the SaeR protein displayed a specific affinity for the P1 promoter fragment. Addition of unlabelled specific DNA abolished the shift (Fig. 1*c*, lane 7), while the nonspecific competitor poly(dI–dC) did not, indicating that the binding of SaeR to the promoter is specific. The EMSA experiments indicated that both SaeR and SaeR^{DBD} could bind to P1 promoter DNA and that SaeR^{DBD} had a lower DNA-binding affinity than the full-length protein. In addition to the previous report that the deletion of residues 1–103 of SaeR may enhance the DNA-binding affinity of SaeR (Sun *et al.*, 2010), the different DNA-binding affinities of the truncations SaeR$^{104–228}$ and SaeR$^{125–228}$ indicated that the loop region consisting of residues 104–124 in SaeR plays an important role in DNA substrate binding or in SaeR domain arrangement.

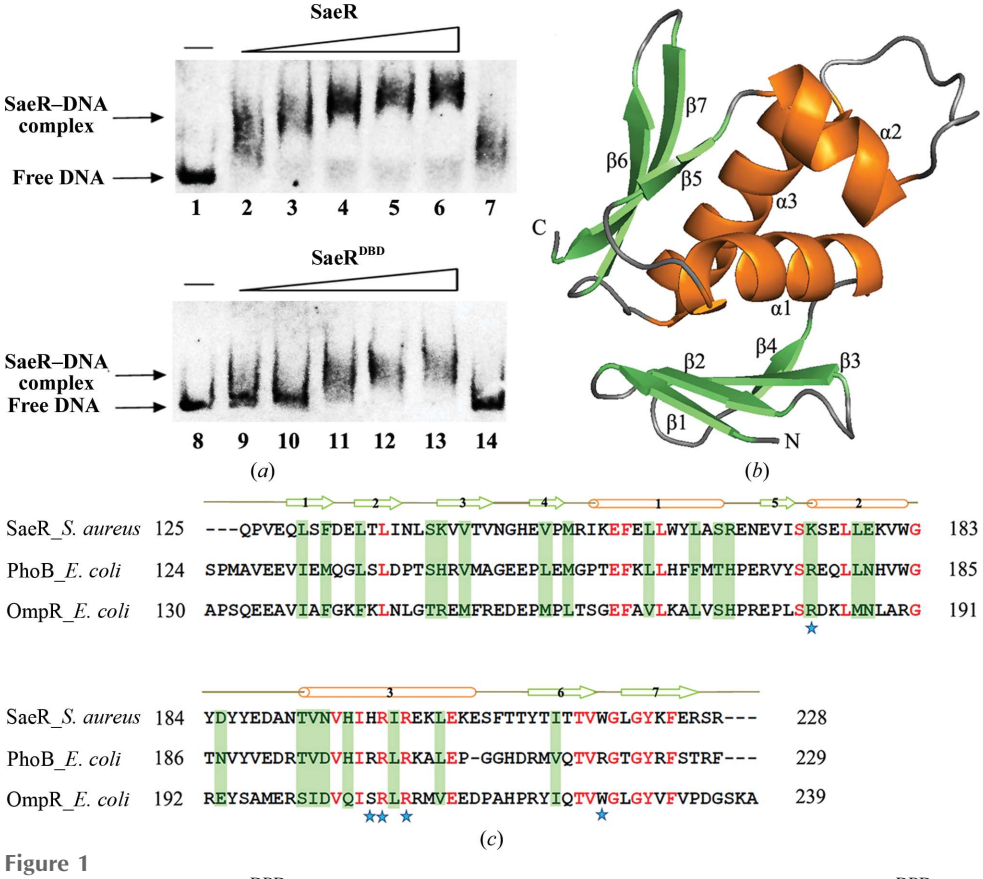

Figure 1
Overall structure of SaeR^{DBD} and its DNA-binding properties. (*a*) EMSA of SaeR and SaeR^{DBD} with biotin-labelled P1 promoter. DNA is at 0.7 n*M* in each lane; the protein in lanes 1–7 is at 0, 36, 54, 72, 90, 108 and 108 µ*M*, respectively; the protein in lanes 8–14 is at 0, 84, 126, 168, 210, 252 and 252 µ*M*, respectively. 7 n*M* cold DNA (unlabelled P1 promoter DNA) was added to lanes 7 and 14. (*b*) Cartoon representation of SaeR^{DBD}. (*c*) Sequence alignment of the DNA-binding domains of SaeR, PhoB and OmpR. The secondary-structural elements of SaeR^{DBD} are shown at the top of the sequence. α-Helices are coloured green and β-strands are coloured orange. Strictly conserved residues and similar residues are depicted in red and green. Residues labelled with a blue star were mutated in this study.

3.2. Overall structure of SaeR^{DBD}

In order to study the mechanism of SaeR as a response regulator, we prepared three recombinant proteins, SaeR, SaeRRD and SaeR^{DBD}, for the growth of crystals. Unfortunately, only the crystals of SaeR^{DBD} diffracted well enough to allow data collection. Details of the data-collection and refinement statistics are summarized in Table 1. The SaeR^{DBD} crystals belonged to space group $P2_12_12_1$ and each asymmetric unit contained two molecules: molecule *A* and molecule *B*. Because of poor electron density, residues 185–188 of molecule *A* of SaeR^{DBD} were not modelled in the final structure. Superposition of the two molecules shows little structural variation [0.619 Å root-mean-square deviation (r.m.s.d); Supplementary Fig. S2*a*]. Molecule *B*, with better electron density in the asymmetric unit, will be discussed in the following. The overall structure of molecule *B* is shown in Fig. 1(*b*). To test

whether SaeR and SaeR^{DBD} exist as a monomer in solution, we performed a size-exclusion chromatographic assay. As shown in Supplementary Fig. S1, SaeR and SaeR^{DBD} eluted with molecular weights of approximately 26.0 and 9.8 kDa, respectively, which were close to the theoretical values for a monomer (26.86 and 12.40 kDa).

SaeR^{DBD} adopts a peach-shaped structure (Fig. 1*b*). It consists of three α-helices and seven β-strands with topology $\beta1$–$\beta2$–$\beta3$–$\beta4$–$\alpha1$–$\beta5$–$\alpha2$–$\alpha3$–$\beta6$–$\beta7$. The $\alpha2$ and $\alpha3$ helices compose the classical helix–turn–helix motif. The C-terminal antiparallel β-strands ($\beta6$–$\beta7$) that form a β-hairpin structure constitute the winged motif. The loop between the $\alpha2$ and $\alpha3$ helices is called the α loop (or the transactivation loop) and interacts with the RNA polymerase (RNAP) subunit to activate transcription, as has been shown in OmpR and PhoB from *E. coli* (Martínez-Hackert & Stock, 1997; Makino *et al.*, 1993). The $\alpha3$ helix is the recognition helix, which is very important for recognizing dsDNA by binding the major

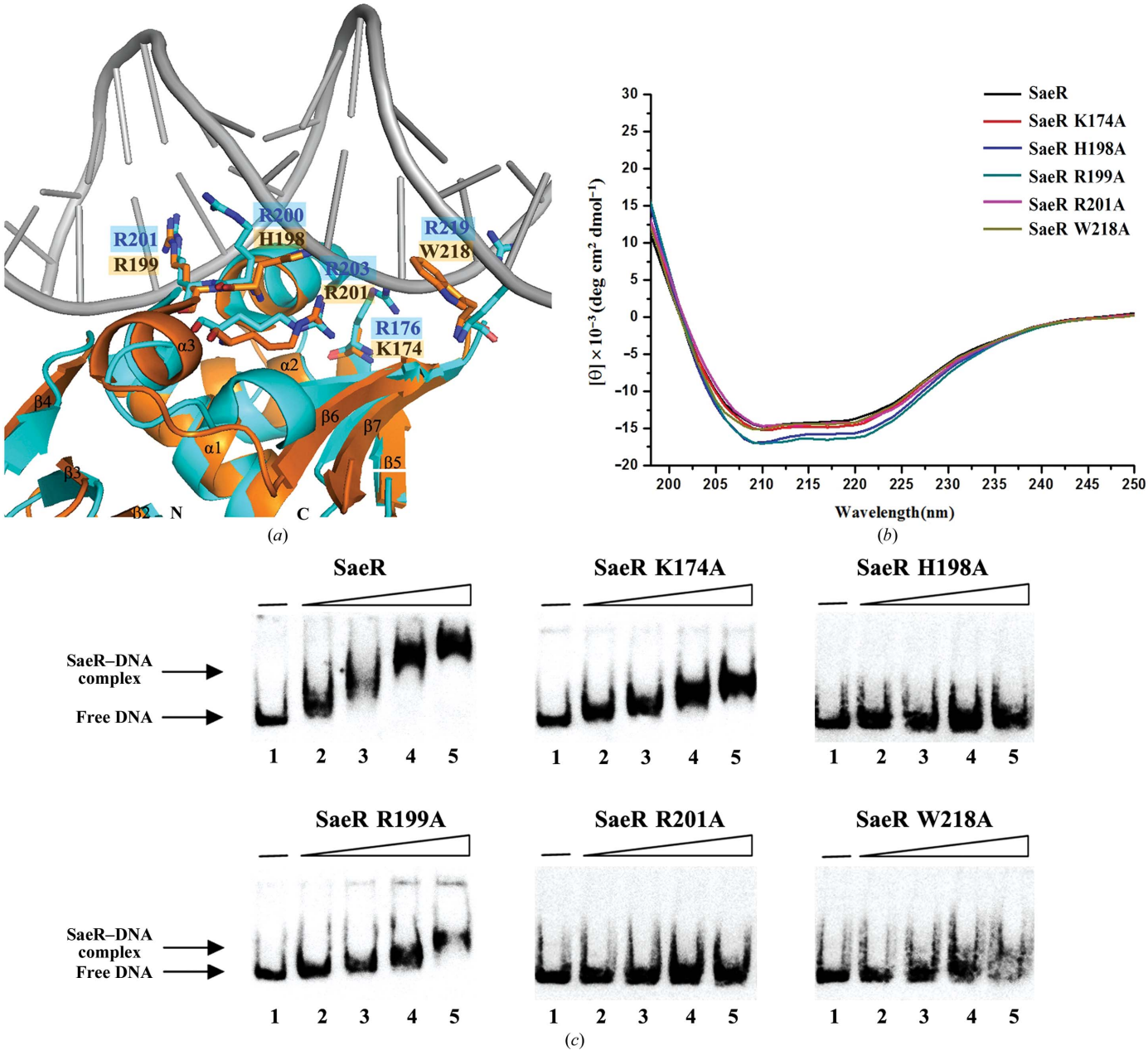

Figure 2
The interaction between SaeR and the P1 promoter. (*a*) Superposition of SaeR^{DBD} onto the structure of PhoB^{DBD}-bound dsDNA (PDB entry 1gxp). Only the winged helix–turn–helix modules of SaeR^{DBD} and molecule *A* of PhoB^{DBD} in 1gxp and part of the dsDNA are shown. Colouring scheme: orange, SaeR^{DBD}; cyan, PhoB^{DBD}; grey, DNA strands. The following side chains of residues of PhoB^{DBD} (the equivalent residues in SaeR ^{DBD} labelled with an orange background are given in parentheses) are shown as sticks: Arg176 (Lys174), Arg200 (His198), Arg201 (Arg199), Arg203 (Arg201) and Arg219 (Trp218). Residues Arg176, Arg200, Arg201, Arg203 and Arg219 are labelled in blue. (*b*) The CD spectra of recombinant SaeR and its mutants. (*c*) EMSA of SaeR and SaeR mutants with biotin-labelled P1 promoter. DNA is at 0.7 n*M*; the protein in lanes 1–5 is at 0, 18, 36, 72 and 108 µ*M*, respectively.

grooves, and the β-hairpin motif contacts the minor grooves, as has been reported in the OmpR/PhoB family (Martínez-Hackert & Stock, 1997; Makino *et al.*, 1993).

3.3. The interaction between SaeR and the P1 promoter

To analyze the interacting surface between $SaeR^{DBD}$ and dsDNA, we superposed $SaeR^{DBD}$ with the $PhoB^{DBD}$–DNA complex (PDB entry 1gxp; Blanco *et al.*, 2002; Fig. 2*a*). Five key residues in the winged helix–turn–helix module were found to have the possibility of interacting with dsDNA. In order to verify that these residues are important for recognizing the target dsDNA, we constructed five SaeR mutants (K174A, H198A, R199A, R201A and W218A) and studied the effects of the various mutations on DNA binding by EMSA. As shown in Fig. 2(*c*), SaeR displayed a high binding affinity for the P1 promoter fragment, while mutations of these residues caused decreased binding affinity. The binding affinity of SaeR H198A, SaeR R201A and SaeR W218A decreased significantly, while the effects of the K174A and R199A mutations were slight. Addition of the nonspecific competitor poly(dI–dC) did not alter the shift, indicating that the binding of SaeR and mutations to the promoter is specific. Sequence alignment showed that with the exception of His198, the other four residues were conserved among SaeR, PhoB and OmpR (Fig. 1*c*). To ascertain that the decreased DNA-binding affinity of these mutant proteins was not owing to abnormal folding behaviour, their secondary structures were determined using circular-dichroism (CD) spectroscopy (Fig. 2*b*). The secondary structures of these mutant proteins were similar to that of the wild-type protein, suggesting that all of the above mutations do not appear to affect the overall protein structure during the recombinant expression process.

3.4. Positive regulation of α-toxin by SaeR

It has been reported that α-toxin is a pore-forming cytotoxin that is upregulated by SaeR (Goerke *et al.*, 2001; Li & Cheung, 2008). The promoter region of α-toxin contains the sequence $GTTAAN_6GTTAA$, which has been shown to be the SaeR binding site (Sun *et al.*, 2010). To confirm that the residues involved in interaction with promoter DNA *in vitro* were also active *in vivo*, we assayed the expression of α-toxin in the wild-type strain, the *saeR* knockout strain NMΔsae and the NMΔsae strain complemented with different SaeR mutants. As shown in Fig. 3(*a*), expression of the α-toxin was obviously detected in the wild-type strain and the SaeR complementary strains, but not in the *saeR* knockout strain NMΔsae. As expected, complementation with SaeR mutants failed to activate expression of the α-toxin except in SaeR H198A, with weak expression. In order to further validate the importance of these residues for the physiological function of *S. aureus*, we analyzed the haemolytic activity of different strains. As shown in Fig. 3(*b*), a high level of haemolytic activity was detected in the wild-type strain and on complementation with SaeR, but not in the knockout strain and on complementation with SaeR mutants, which was in agreement with the Western blot results for the α-toxin. For SaeR H198A, with weak expression of α-toxin, we also did not observe haemolytic activity. We speculated that the Western blot assay is more sensitive and the amount of α-toxin was not sufficient to reach the threshold of the haemolytic activity assay. Two mutations (K174A and R199A) had a slight influence on the *in vitro* DNA binding of SaeR but impacted greatly on *in vivo* α-toxin expression, while the H198A mutation abolished DNA binding *in vitro* but showed detectable α-toxin in a Western blot assay. These suggest that the binding between the P1 promoter and the α-toxin promoter may be different and there may be other layers of regulation of α-toxin gene expression.

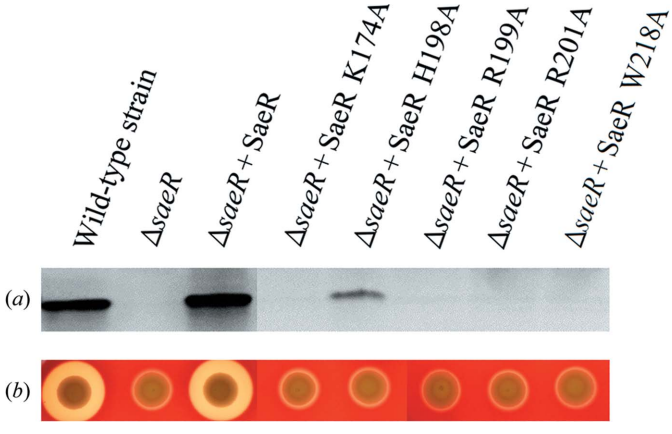

Figure 3
Functional analysis of *S. aureus* Newman strain (wild-type strain), the *saeR* knockout strain and complementary strains with SaeR and SaeR mutants *in vivo*. (*a*) Western blot analysis of the α-toxin. (*b*) Haemolysis on sheep blood agar. Clear zones indicate haemolytic activity.

3.5. Putative $SaeR^{DBD}$–dsDNA recognition model

Blanco and coworkers reported the crystal structure of $PhoB^{DBD}$ in complex with its target DNA, in which two $PhoB^{DBD}$ molecules bind in tandem to the DNA moiety (Blanco *et al.*, 2002). Subsequently, Narayanan and coworkers presented the structure of full-length KdpE, a member of the OmpR/PhoB family, bound to 30 bp dsDNA, in which two KdpE molecules form a asymmetric dimer in an active-like conformation without phosphorylation (Narayanan *et al.*, 2014). We compared $SaeR^{DBD}$ with the DNA-binding domains of PhoB (PDB entry 1gxq; Blanco *et al.*, 2002) and OmpR (PDB entry 1opc; Martínez-Hackert & Stock, 1997), which showed similar overall structures with C^{α} r.m.s.d.s from 1.863 Å (96 C^{α} atoms) to 3.926 Å (74 C^{α} atoms) (Supplementary Figs. S2*c* and S2*d*). The r.m.s.d. of the winged helix–turn–helix module between $SaeR^{DBD}$ and $OmpR^{DBD}$ was 4.095 Å for 52 comparable C^{α} atoms, while the winged helix–turn–helix modules of $SaeR^{DBD}$ and $PhoB^{DBD}$ were more similar, with an r.m.s.d for 51 C^{α} atoms of 2.181 Å. Based on the high sequence identity (31.8%) and structural similarity between $SaeR^{DBD}$ and $PhoB^{DBD}$, we speculated that $SaeR^{DBD}$ recognized the P1 promoter with the helix–turn–helix motif and β-hairpin motif, which is similar to the DNA-binding model of $PhoB^{DBD}$. We also confirmed that five residues in the winged helix–turn–helix module were important for binding to

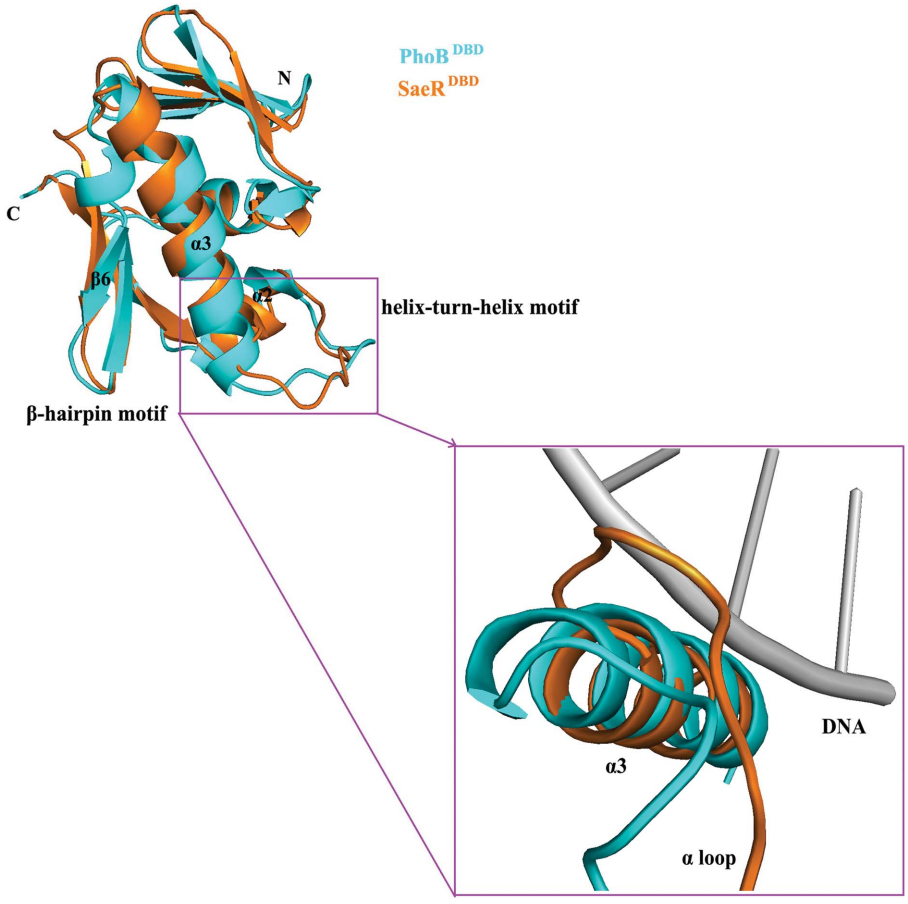

Figure 4
Structural superposition of the DNA-binding domains of SaeR and PhoB. SaeR is in orange; PhoB (PDB entry 1gxq) is in cyan. The close-up view highlights the difference in the mode of binding to dsDNA of the α loop in SaeR and PhoB. DNA in the structure of the PhoB–DNA complex (PDB entry 1gxp) is shown in grey.

the P1 promoter *in vitro* and for the physiological function *in vivo*. Little difference between SaeR^{DBD} and PhoB^{DBD} in interacting with dsDNA was found on comparing their structures. The largest backbone deviations occur in the loop regions α2–α3 (α loop) and α3–β6 (Fig. 4). The α loop of SaeR^{DBD} has a unique structure, with the first half turn of the α3 helix unwound compared with PhoB^{DBD}. As shown in the close-up view in Fig. 4, this conformation will result in steric clashes between the α loop and the DNA if the recognition helix of SaeR^{DBD} binds to the dsDNA in a similar manner as in PhoB^{DBD}. However, owing to the flexibility of the loop, it is possible that the conformation of the α loop will change once it binds to its target dsDNA. By comparing the surface electrostatic potential between SaeR^{DBD} and PhoB^{DBD}, the C-terminus of the α2 helix and the N-terminus of the α3 helix in SaeR^{DBD} have a positive electrostatic potential and the rest of the molecular surface is either negatively charged or neutral, while PhoB^{DBD} has an alkaline patch at a similar position (Fig. 5). The C-terminal β-hairpin turn of SaeR^{DBD} has a neutral electrostatic potential, while the corresponding turn of PhoB^{DBD} is highly positively charged. The DNA-binding patch electrostatic

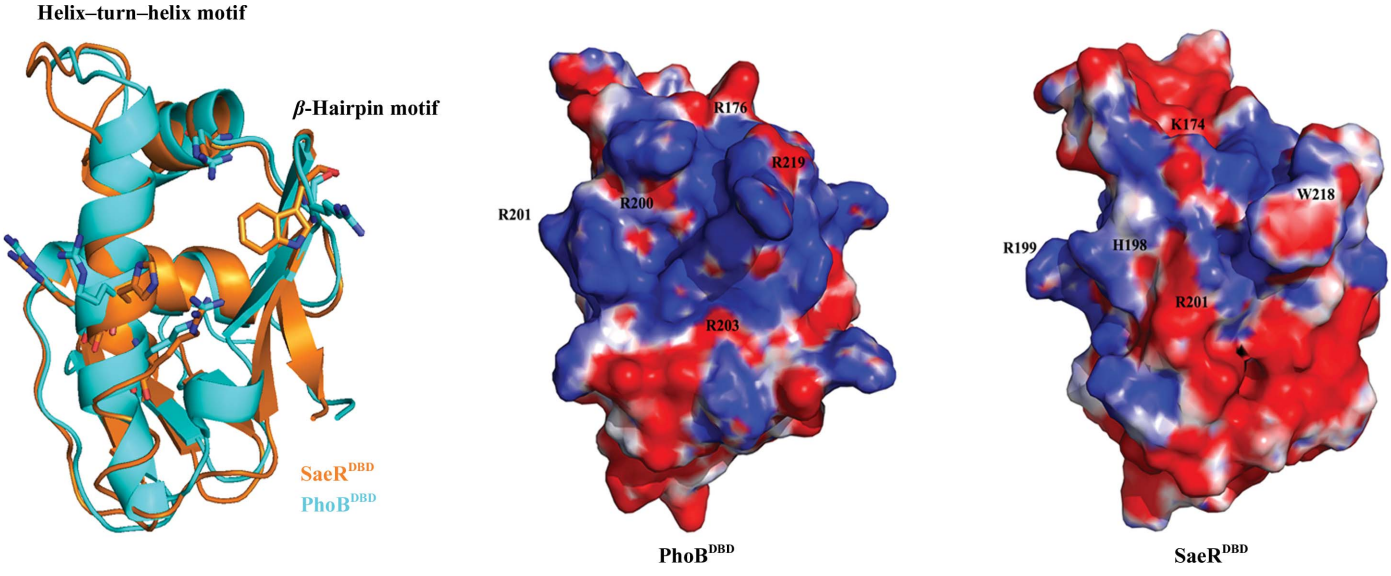

Figure 5
Surface view of the electrostatic potentials of SaeR^{DBD} and PhoB^{DBD}. SaeR^{DBD} is in orange and PhoB^{DBD} is in cyan. Residues interacting with DNA are shown as sticks (left figure).

potential differences between SaeR^{DBD} and PhoB^{DBD} indicate that the DNA-binding details of these two proteins would be somewhat different.

SaeR^{DBD} and PhoB^{DBD} have a similar acidic patch built up by the transactivation loop and the α2 helix. This patch on the PhoB^{DBD} surface has been reported to interact with the RNAP subunit (Blanco *et al.*, 2011), and P-SaeR also can bind to the RNAP subunit to activate transcription at the promoter (Sun *et al.*, 2010; Cho *et al.*, 2012). Therefore, we speculated that SaeR^{DBD} could interact with the RNAP subunit in a similar manner as PhoB^{DBD}. However, further studies will be needed to demonstrate the details of how SaeR interacts with the RNAP subunit to activate transcription of the target promoters.

Acknowledgements

We thank the staff of BL17U at SSRF for assistance with synchrotron diffraction data collection and thank Dr Taeok Bae for providing the NMΔsae strain. Financial support for this project was provided by the Chinese National Natural Science Foundation (Grant No. 31130018), the Chinese Ministry of Science and Technology (Grant No. 2012CB917200), the Chinese National Natural Science Foundation (Grant Nos. 31370732 and 31270014) and the Science and Technological Fund of Anhui Province for Outstanding Youth (Grant No. 1308085JGD08).

References

Adams, P. D. *et al.* (2010). *Acta Cryst.* D**66**, 213–221.
Adem, P. V., Montgomery, C. P., Husain, A. N., Koogler, T. K., Arangelovich, V., Humilier, M., Boyle-Vavra, S. & Daum, R. S. (2005). *N. Engl. J. Med.* **353**, 1245–1251.
Arumugaswami, V. *et al.* (2009). *J. Virol.* **83**, 1811–1822.
Arvidson, S. & Tegmark, K. (2001). *Int. J. Med. Microbiol.* **291**, 159–170.
Bachhawat, P. & Stock, A. M. (2007). *J. Bacteriol.* **189**, 5987–5995.
Bachhawat, P., Swapna, G. V., Montelione, G. T. & Stock, A. M. (2005). *Structure*, **13**, 1353–1363.
Barrett, J. F. & Hoch, J. A. (1998). *Antimicrob. Agents Chemother.* **42**, 1529–1536.
Bischoff, M., Dunman, P., Kormanec, J., Macapagal, D., Murphy, E., Mounts, W., Berger-Bächi, B. & Projan, S. (2004). *J. Bacteriol.* **186**, 4085–4099.
Blanco, A. G., Canals, A., Bernués, J., Solà, M. & Coll, M. (2011). *EMBO J.* **30**, 3776–3785.
Blanco, A. G., Sola, M., Gomis-Rüth, F. X. & Coll, M. (2002). *Structure*, **10**, 701–713.
Brunskill, E. W. & Bayles, K. W. (1996). *J. Bacteriol.* **178**, 611–618.
Buckler, D. R., Zhou, Y. & Stock, A. M. (2002). *Structure*, **10**, 153–164.
Chen, V. B., Arendall, W. B., Headd, J. J., Keedy, D. A., Immormino, R. M., Kapral, G. J., Murray, L. W., Richardson, J. S. & Richardson, D. C. (2010). *Acta Cryst.* D**66**, 12–21.
Cheung, A. L., Nishina, K. A., Trotonda, M. P. & Tamber, S. (2008). *Int. J. Biochem. Cell Biol.* **40**, 355–361.
Cheung, A. L. & Ying, P. (1994). *J. Bacteriol.* **176**, 580–585.
Cho, H., Jeong, D.-W., Li, C. & Bae, T. (2012). *J. Bacteriol.* **194**, 2865–2876.
Cosgrove, S. E., Carroll, K. C. & Perl, T. M. (2004). *Clin. Infect. Dis.* **39**, 539–545.
Emsley, P. & Cowtan, K. (2004). *Acta Cryst.* D**60**, 2126–2132.
Fournier, B., Klier, A. & Rapoport, G. (2001). *Mol. Microbiol.* **41**, 247–261.
Friedland, N., Mack, T. R., Yu, M., Hung, L.-W., Terwilliger, T. C., Waldo, G. S. & Stock, A. M. (2007). *Biochemistry*, **46**, 6733–6743.
Galperin, M. Y. (2006). *J. Bacteriol.* **188**, 4169–4182.
Gardete, S., Wu, S. W., Gill, S. & Tomasz, A. (2006). *Antimicrob. Agents Chemother.* **50**, 3424–3434.
Geiger, T., Goerke, C., Mainiero, M., Kraus, D. & Wolz, C. (2008). *J. Bacteriol.* **190**, 3419–3428.
Gillet, Y., Issartel, B., Vanhems, P., Fournet, J.-C., Lina, G., Bes, M., Vandenesch, F., Piémont, Y., Brousse, N., Floret, D. & Etienne, J. (2002). *Lancet*, **359**, 753–759.
Giraudo, A. T., Calzolari, A., Cataldi, A. A., Bogni, C. & Nagel, R. (1999). *FEMS Microbiol. Lett.* **177**, 15–22.
Giraudo, A. T., Cheung, A. L. & Nagel, R. (1997). *Arch. Microbiol.* **168**, 53–58.
Giraudo, A. T., Raspanti, C. G., Calzolari, A. & Nagel, R. (1994). *Can. J. Microbiol.* **40**, 677–681.
Goerke, C., Fluckiger, U., Steinhuber, A., Bisanzio, V., Ulrich, M., Bischoff, M., Patti, J. M. & Wolz, C. (2005). *Infect. Immun.* **73**, 3415–3421.
Goerke, C., Fluckiger, U., Steinhuber, A., Zimmerli, W. & Wolz, C. (2001). *Mol. Microbiol.* **40**, 1439–1447.
Harraghy, N., Kormanec, J., Wolz, C., Homerova, D., Goerke, C., Ohlsen, K., Qazi, S., Hill, P. & Herrmann, M. (2005). *Microbiology*, **151**, 1789–1800.
Hiron, A., Falord, M., Valle, J., Débarbouillé, M. & Msadek, T. (2011). *Mol. Microbiol.* **81**, 602–622.
Hoch, J. A. (2000). *Curr. Opin. Microbiol.* **3**, 165–170.
Jeong, D.-W., Cho, H., Lee, H., Li, C., Garza, J., Fried, M. & Bae, T. (2011). *J. Bacteriol.* **193**, 4672–4684.
King-Scott, J., Nowak, E., Mylonas, E., Panjikar, S., Roessle, M., Svergun, D. I. & Tucker, P. A. (2007). *J. Biol. Chem.* **282**, 37717–37729.
Laskowski, R. A., MacArthur, M. W., Moss, D. S. & Thornton, J. M. (1993). *J. Appl. Cryst.* **26**, 283–291.
Li, D. & Cheung, A. (2008). *Infect. Immun.* **76**, 1068–1075.
Lowy, F. D. (1998). *N. Engl. J. Med.* **339**, 520–532.
Makino, K., Amemura, M., Kim, S.-K., Nakata, A. & Shinagawa, H. (1993). *Genes Dev.* **7**, 149–160.
Martínez-Hackert, E. & Stock, A. M. (1997). *Structure*, **5**, 109–124.
Menon, S. & Wang, S. (2011). *Biochemistry*, **50**, 5948–5957.
Miller, L. G., Perdreau-Remington, F., Rieg, G., Mehdi, S., Perlroth, J., Bayer, A. S., Tang, A. W., Phung, T. O. & Spellberg, B. (2005). *N. Engl. J. Med.* **352**, 1445–1453.
Morfeldt, E., Tegmark, K. & Arvidson, S. (1996). *Mol. Microbiol.* **21**, 1227–1237.
Murshudov, G. N., Skubák, P., Lebedev, A. A., Pannu, N. S., Steiner, R. A., Nicholls, R. A., Winn, M. D., Long, F. & Vagin, A. A. (2011). *Acta Cryst.* D**67**, 355–367.
Narayanan, A., Kumar, S., Evrard, A. N., Paul, L. N. & Yernool, D. A. (2014). *Nature Commun.* **5**, 3282.
Narayanan, A., Paul, L. N., Tomar, S., Patil, D. N., Kumar, P. & Yernool, D. A. (2012). *PLoS One*, **7**, e30102.
Novick, R. P. & Jiang, D. (2003). *Microbiology*, **149**, 2709–2717.
Nowak, E., Panjikar, S., Konarev, P., Svergun, D. I. & Tucker, P. A. (2006). *J. Biol. Chem.* **281**, 9659–9666.
Otwinowski, Z. & Minor, W. (1997). *Method Enzymol.* **276**, 307–326.
Robinson, V. L., Wu, T. & Stock, A. M. (2003). *J. Bacteriol.* **185**, 4186–4194.
Steinhuber, A., Goerke, C., Bayer, M. G., Döring, G. & Wolz, C. (2003). *J. Bacteriol.* **185**, 6278–6286.
Stephenson, K. & Hoch, J. A. (2002). *Curr. Opin. Pharmacol.* **2**, 507–512.
Stock, A. M., Robinson, V. L. & Goudreau, P. N. (2000). *Annu. Rev. Biochem.* **69**, 183–215.
Sun, F., Li, C., Jeong, D., Sohn, C., He, C. & Bae, T. (2010). *J. Bacteriol.* **192**, 2111–2127.

Toro-Roman, A., Mack, T. R. & Stock, A. M. (2005). *J. Mol. Biol.* **349**, 11–26.
Vagin, A. & Teplyakov, A. (2010). *Acta Cryst.* D**66**, 22–25.
Wang, S., Engohang-Ndong, J. & Smith, I. (2007). *Biochemistry-Us* **46**, 14751–14761.
West, A. H. & Stock, A. M. (2001). *Trends Biochem. Sci.* **26**, 369–376.
Winn, M. D. *et al.* (2011). *Acta Cryst.* D**67**, 235–242.
Wuichet, K., Cantwell, B. J. & Zhulin, I. B. (2010). *Curr. Opin. Microbiol.* **13**, 219–225.
Xue, T., You, Y., Hong, D., Sun, H. & Sun, B. (2011). *Infect. Immun.* **79**, 2154–2167.
Xue, T., Zhang, X., Sun, H. & Sun, B. (2014). *Med. Microbiol. Immunol.* **203**, 1–12.
Zhu, Y., Fan, X., Zhang, X., Jiang, X., Niu, L., Teng, M. & Li, X. (2014). *Acta Cryst.* D**70**, 2467–2476.